

# Hybridization of DNA to Bead-Immobilized Probes Confined within a Microfluidic Channel

Jooheon Kim, Jinseok Heo,<sup>†</sup> and Richard M. Crooks\*

Department of Chemistry and Biochemistry, The University of Texas at Austin, 1 University Station, A5300, Austin, Texas 78712-0165

Received June 13, 2006. In Final Form: September 4, 2006

We report the factors influencing the capture of DNA by DNA-modified microbeads confined within a microfluidic channel. Quantitative correlation of target capture efficiency to probe surface concentration, solution flow rate, and target concentration are discussed. The results indicate that the microfluidic system exhibits a limit of detection of  $\sim 10^{-10}$  M ( $\sim 10^{-16}$  mol) DNA and a selectivity factor of  $\sim 8 \times 10^3$ . Typical hybridization times are on the order of minutes.

## Introduction

Here we report an investigation of parameters influencing the hybridization of DNA onto probe-conjugated microbeads confined within a microfluidic channel. The use of beads as supports for capture probes in microfluidic systems is advantageous for a number of reasons. First, the bead surface area is significantly larger than the interior surface area of a typical microfluidic channel, and this results in enhanced sensitivity and limit of detection for assays based on immobilized capture probes.<sup>1–3</sup> Second, in addition to providing a platform for probe attachment, beads also effectively mix solutions in microfluidic systems.<sup>3</sup> Third, it is easier to modify and characterize the surface of beads than the walls of a microfluidic device.<sup>4,5</sup> Because of the importance of these three points, it makes sense to develop a better understanding of the conditions that lead to target capture on bead surfaces. Accordingly, we have studied capture efficiency in terms of target concentration, probe surface concentration, and flow rate within the microfluidic channel.

We previously reported on fluorescence-based methods for studying bio/chemical reactions on functionalized beads immobilized within microfluidic channels.<sup>3,6</sup> For example, we demonstrated that multiple, sequential catalytic reactions could be carried out in this format by immobilizing catalytic enzymes on microbeads, placing the beads into microreactors, and then passing reactants through one or more of these reactors to yield products. The enzyme-modified beads mixed reactants and increased the effective surface area of the channel interior, both of which improved reaction velocities compared to open channels.<sup>3</sup> We also demonstrated efficient DNA hybridization on DNA-functionalized microbeads packed in a serial microchamber array. Hybridization, which was 90% complete within 1 min, was carried out by moving multiple DNA targets across

the microbead array by electrophoresis.<sup>6</sup> These types of experiments demonstrate the viability of this general approach for bead-based microfluidic assays, but until now we have not provided quantitative insight into the factors that control the efficiency of such devices.

In addition to our own reports, a number of other groups have also been actively studying bead-based microanalytical systems. For example, DNA hybridization using paramagnetic beads modified with targets was demonstrated in a microfluidic array format.<sup>7</sup> A capillary platform for DNA analysis was prepared by lining up individual beads, each modified with a different probe sequence, within a capillary having approximately the same inside diameter as the bead outer diameter.<sup>8,9</sup> A chip-based sensor array composed of individually addressable microbeads and having point mutation selectivity has also been demonstrated.<sup>10</sup> There are a number of other interesting studies of bead-based microfluidic biosensors.<sup>11–14</sup>

In the present study, experimental factors controlling the hybridization of DNA onto probe-conjugated microbeads under microfluidic flow conditions are reported. Specifically, streptavidin-coated microbeads were conjugated with biotinylated single-strand (ss) DNA probes. The density of probe ssDNA on the microbeads ( $1.9 \times 10^{12}$  probes/cm<sup>2</sup>) was controlled to be within the range that leads to rapid hybridization.<sup>15–17</sup> The probe-conjugated microbeads are sufficiently closely packed in the microfluidic channel that mass transfer from solution to the bead surface is significantly enhanced compared to the corresponding open channel. A limit of detection (LOD) of  $\sim 10^{-10}$  M ssDNA

\* To whom correspondence should be addressed: phone 512-475-8674; fax 512-475-8651; e-mail crooks@cm.utexas.edu.

<sup>†</sup> Present address: Department of Mechanical and Aerospace Engineering, The State University of New York at Buffalo, Buffalo, NY 14260.

(1) Zammattio, N.; Alexandre, I.; Ernest, I.; Le, L.; Brancart, F.; Remacle, J. *Anal. Biochem.* **1997**, *253*, 180–189.

(2) Sato, K.; Tokeshi, M.; Odake, T.; Kimura, H.; Ooi, T.; Nakao, M.; Kitamori, T. *Anal. Chem.* **2000**, *72*, 1144–1147.

(3) Seong, G. H.; Crooks, R. M. *J. Am. Chem. Soc.* **2002**, *124*, 13360–13361.

(4) Huang, S.; Stump, M. D.; Weiss, R.; Caldwell, K. D. *Anal. Biochem.* **1996**, *237*, 115–122.

(5) Walsh, M. K.; Wang, X.; Weimer, B. C. *J. Biochem. Biophys. Methods* **2001**, *47*, 221–231.

(6) Seong, G. H.; Zhan, W.; Crooks, R. M. *Anal. Chem.* **2002**, *74*, 3372–3377.

(7) Fan, Z. H.; Mangru, S.; Granzow, R.; Heaney, P.; Ho, W.; Dong, Q.; Kumar, R. *Anal. Chem.* **1999**, *71*, 4851–4859.

(8) Kohara, Y.; Noda, H.; Okano, K.; Kambara, H. *Nucleic Acids Res.* **2002**, *30*, e87.

(9) Kohara, Y. *Anal. Chem.* **2003**, *75*, 3079–3085.

(10) Ali, M. F.; Kirby, R.; Goodey, A. P.; Rodriguez, M. D.; Ellington, A. D.; Neikirk, D. P.; McDevitt, J. T. *Anal. Chem.* **2003**, *75*, 4732–4739.

(11) Kwakye, S.; Baeumner, A. *Anal. Bioanal. Chem.* **2003**, *376*, 1062–1068.

(12) Gabig-Ciminska, M.; Holmgren, A.; Andresen, H.; Bundvig Barken, K.; Wümpelmann, M.; Albers, J.; Hintsche, R.; Breitenstein, A.; Neubauer, P.; Los, M.; Czyn, A.; Wegrzyn, G.; Silfversparre, G.; Jürgen, B.; Schweder, T.; Enfors, S.-O. *Biosens. Bioelectron.* **2004**, *19*, 537–546.

(13) Smistrup, K.; Kjeldsen, B. G.; Reimers, J. L.; Dufva, M.; Petersen, J.; Hansen, M. F. *Lab Chip* **2005**, *5*, 1315–1319.

(14) Goral, V. N.; Zaytseva, N. V.; Baeumner, A. J. *Lab Chip* **2006**, *6*, 414–421.

(15) Herne, T. M.; Tarlov, M. J. *J. Am. Chem. Soc.* **1997**, *119*, 8916–8920.

(16) Steel, A. B.; Herne, T. M.; Tarlov, M. J. *Anal. Chem.* **1998**, *70*, 4670–4677.

(17) Peterson, A. W.; Heaton, R. J.; Georgiadis, R. M. *Nucleic Acids Res.* **2001**, *29*, 5163–5168.

( $\sim 10^{-16}$  mol) was obtained. The hybridization time was on the order of a few minutes and the selectivity factor was greater than  $8 \times 10^3$ . Typically,  $\sim 2 \mu\text{L}$  volume of solution was required for an analysis. We expect this simple microfluidic system to complement the use of planar DNA arrays<sup>18–20</sup> and to be particularly useful for applications requiring fast response and simplicity.

### Experimental Section

**Materials.** DNA oligonucleotides modified with biotin or fluorescein (probes or targets) were used as received from Integrated DNA Technologies (Coralville, IA). Tris–acetate/ethylenediamine-tetraacetic acid (TAE) buffer (pH 8.0; 40 mM Tris–acetate, 1.0 mM EDTA, and 0.5 M NaCl) and hybridization buffer (Perfecthyb Plus) solutions were obtained from the Sigma–Aldrich Co. (St. Louis, MO). The hybridization buffer solution was diluted by a factor of 2 with water prior to use. TAE buffer was used for rinsing bead beds after hybridization. Milli-Q water (18 M $\Omega$ ·cm, Millipore, Bedford, MA) was used throughout. The sequences of 5′-biotin-modified probe and 5′-fluorescein-labeled targets are as follows:<sup>21</sup> ssDNA probe, 5′ (biotin-TEG) AGT TGA GGG GAC TTT CCC AGG C 3′; ssDNA complementary target, 5′ (6-FAM) GCC TGG GAA AGT CCC CTC AAC T 3′; ssDNA noncomplementary target, 5′ (6-FAM) CTA GAA TCG CTG ATT ACA GCT T 3′.

**Fabrication of Microfluidic Devices.** Microfluidic devices were fabricated under clean-room conditions, as previously described, but with some modifications.<sup>6</sup> Briefly, positive photoresist (AZP4620, Clariant Co., Somerville, NJ) was spin-coated twice onto a glass substrate (Fisher Scientific, Pittsburgh, PA) at 1500 rpm for 2 min, followed by soft baking at 92 °C for 5 min on a hot plate. The photoresist-coated glass substrate was exposed to UV light for 2 min by use of a mask aligner (Q 4000-6, Quintel Corp., San Jose, CA) and a photographic film mask. The resulting image was then developed with 100% AZ421K solution (Clariant Co.) to yield a photoresist master. Next, the master was exposed to UV light again for 1 min through a slit-type, chrome-coated soda lime glass mask (Nanofilm, Westlake Village, CA) having a slit width of 100  $\mu\text{m}$ . The master was developed again in a 75% AZ421K/25% water (v/v) solution for 1 min, which resulted in formation of a weir structure on the master. The depth and width of the resulting microstructures were measured with a profilometer (Veeco Dektak 3, Veeco Instruments, Plainview, NY).

PDMS (Sylgard 184, Dow Corning, Midland, MI) was molded against the photoresist master to yield the microfluidic device. The PDMS replica and a cover glass were then oxidized in a plasma cleaner/sterilizer (PDC-32G, Harrick Scientific, Ossining, NY) at medium power for 25 s. Immediately after the plasma treatment, they were brought into conformal contact and permanently sealed together.<sup>22,23</sup>

**Preparation and Characterization of Probe-Conjugated Microbeads.** Biotinylated ssDNA probe oligonucleotides were conjugated to SuperAvidin-coated microbeads (ProActive Microspheres, diameter 9.95  $\mu\text{m}$ ; Bangs Laboratories Inc., Fishers, IN) by the following procedure. First, 15  $\mu\text{L}$  of stock microbeads ( $1.8 \times 10^4$  beads/ $\mu\text{L}$ ) were rinsed in phosphate-buffered saline (PBS) solution containing 0.05% (v/v) Tween 20 (pH 7.4; 0.15 M NaCl, 4.0 mM KCl, 8.1 mM Na<sub>2</sub>HPO<sub>4</sub>, and 1.5 mM KH<sub>2</sub>PO<sub>4</sub>) and then centrifuged at 4000 rpm for 3 min. Second, 4.0  $\mu\text{L}$  of the biotinylated ssDNA

probe solution (5.0  $\mu\text{M}$ ), which corresponds to a 5-fold excess relative to the binding capacity of the microbeads, was added to the rinsed microbead pellet. This solution was gently mixed for 30 min at  $25 \pm 2$  °C. After conjugation, the mixture was centrifuged to remove unbound biotinylated ssDNA probes. The probe-conjugated microbead pellet was rinsed with PBS buffer solution and centrifuged again. The probe-conjugated microbeads were resuspended in TAE buffer ( $5.4 \times 10^2$  beads/ $\mu\text{L}$ ) and refrigerated (2 °C) until needed.

To estimate the probe density on the microbeads, ssDNA probes, which were modified with fluorescein and biotin at the 3′ and 5′ ends, respectively, were immobilized on microbeads by the previously described method, except all rinsing solutions were collected during the conjugation process. An additional filtering step (0.22  $\mu\text{m}$  syringe filter, Millex-GV13, Sigma–Aldrich Co., St. Louis, MO) was performed with the rinsed microbeads to ensure collection of all unbound, ssDNA probes. The amount of unbound probe DNA was estimated by comparing the fluorescence from the retrieved probe solution to standards. The amount of immobilized probe DNA was calculated from the difference between the initially added DNA and the free DNA in solution. A fluorescence spectrometer (SLM-Aminco spectrofluorometer, Jobin Yvon Inc., Edison, NJ) with excitation and emission wavelengths of 494 and 518 nm, respectively, was used to measure the fluorescence intensity of solutions.

**DNA Hybridization.** Probe-conjugated microbeads were packed in the microfluidic chambers with a syringe pump (PHD 2000, Harvard Apparatus, Holliston, MA), and then the microchambers were extensively rinsed with hybridization buffer for 10 min. Hybridization experiments were performed by flowing fluorescein-labeled ssDNA over the beads at  $25 \pm 2$  °C, rinsing with TAE buffer, and then measuring the resulting fluorescence. A fluorescence microscope (Nikon Eclipse TE 300, Nikon Co., Tokyo, Japan) equipped with band-pass filters, a 100 W mercury lamp, and a charge-coupled device (CCD) camera (Photometrics Ltd., Tucson, AZ) was used to acquire optical and fluorescence micrographs of the microchambers. Micrographs were obtained with a 4 $\times$  or 10 $\times$  objective lens (numerical apertures 0.10 or 0.30, respectively). The integration times for the CCD camera were 1 and 700 ms for optical and fluorescence micrographs, respectively. Micrographs were processed with V++ Precision Digital Imaging software (Digital Optics, Auckland, New Zealand). Fluorescence intensities were measured in the center regions of the bead-packed microchambers (40  $\times$  205 pixels). Background fluorescence intensities were acquired before flowing of the target solution and subtracted from micrographs obtained after flowing of the targets and rinsing of the beads with buffer. For hybridization efficiency experiments, the subtracted intensity was normalized to the maximum hybridization intensity obtained after flowing of a relatively concentrated target solution (1.0  $\mu\text{M}$ ) over the bead bed for 10 min at a flow rate of 1.00  $\mu\text{L}/\text{min}$  and then rinsing for 10 min at a flow rate of 1.00  $\mu\text{L}/\text{min}$ . The average and standard deviation were obtained with three independently prepared microfluidic devices.

### Results and Discussion

**Microfluidic Devices.** As discussed in the Experimental Section, the microfluidic devices used in this study were fabricated by standard photolithographic techniques.<sup>22,23</sup> Microbeads were introduced into the microchambers by pressure-driven flow and retained there by the presence of weirs. Figure 1a is a schematic illustration of the cross section of a microchip, and Figure 1b is a top-view optical micrograph of a microchamber packed with beads. The height of the microchannels was  $21 \pm 2 \mu\text{m}$ . The height of weirs ranged from 5 to 8  $\mu\text{m}$  and depended on the UV exposure time, the concentration of resist developer, and the resist development time. To ensure reproducible packing of the microbeads, a fixed concentration of beads ( $5.4 \times 10^2$  beads/ $\mu\text{L}$ ) and solution flow rate (10.00  $\mu\text{L}/\text{min}$ ) were used. Microbead packing was completed in <30 s (Supporting Information, Movie S1). Each microchamber typically contained about  $2 \times 10^3$

(18) Lemieux, B.; Aharoni, A.; Schena, M. *Mol. Breed.* **1998**, *4*, 277–289.

(19) Gerhold, D.; Rushmore, T.; Caskey, C. T. *Trends Biochem. Sci.* **1999**, *24*, 168–173.

(20) Marx, J. *Science* **2000**, *289*, 1670–1672.

(21) For DNA hybridization experiments with different concentrations of target solution, the following sequences of probes and targets were used to avoid quenching of fluorescein due to a proximal guanine base. ssDNA probe, 5′ (biotin-TEG) CGT TGA GGG GAC TTT CCC AGG C 3′; ssDNA complementary target, 5′ (6-FAM) TCC TGG GAA AGT CCC CTC AAC T 3′.

(22) Duffy, D. C.; McDonald, J. C.; Schueller, O. J. A.; Whitesides, G. M. *Anal. Chem.* **1998**, *70*, 4974–4984.

(23) McDonald, J. C.; Duffy, D. C.; Anderson, J. R.; Chiu, D. T.; Wu, H.; Schueller, O. J. A.; Whitesides, G. M. *Electrophoresis* **2000**, *21*, 27–40.

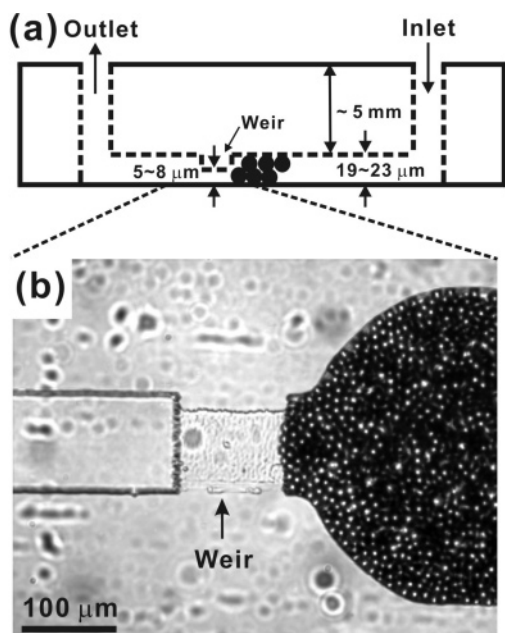


**Figure 1.** (a) Schematic cross-section of the microchip design used for all experiments (not to scale). (b) Optical micrograph of a weir and the corresponding microchamber packed with  $9.95 \mu\text{m}$  diameter microbeads.

microbeads,<sup>24</sup> which corresponds to a packing efficiency, defined as the total bead volume/microchamber volume, of about 0.8. This unusually high value probably arises because of a slight pressure-induced expansion of the PDMS microchamber.<sup>25</sup> Consistent with this view, we observed microbeads (diameter  $9.95 \mu\text{m}$ ) packed up to three layers thick near the center region of the microchambers, even though the measured height (at zero pressure) was only sufficient to accommodate two beads.

**Probe Density.** To determine the density of DNA on the microbead surface, the beads were exposed to an excess of biotinylated DNA labeled with fluorescein (see Experimental Section). After immobilization of a fraction of this excess, the remaining free DNA was retrieved and quantified by measuring the fluorescence of the resulting solution (Supporting Information, Figure S1). The measured probe density was  $(1.0 \pm 0.4) \times 10^{-17}$  mol/microbead or  $1.9 \times 10^{12}$  probes/cm<sup>2</sup> of bead surface area. When the total number of streptavidin binding sites on the surface of the beads is considered, this value corresponds to a DNA binding efficiency of 73%.<sup>26</sup>

There is an optimal surface-probe density for maximum DNA hybridization efficiency.<sup>15–17</sup> At surface densities higher than this optimal value, repulsive electrostatic interactions and steric hindrance between oligonucleotides reduce hybridization efficiency. The calculated maximum density of 22-mer duplex DNA lying flat on the surface of a microbead is  $6.7 \times 10^{12}$  molecules/cm<sup>2</sup>.<sup>16,27,28</sup> This value is about 3 times larger than the measured probe DNA density of  $1.9 \times 10^{12}$  probes/cm<sup>2</sup>, suggesting that electrostatic and steric barriers to hybridization

(24) Calculated value (number of beads/ $\mu\text{L}$   $\times$  flow rate  $\times$  packing time) with the assumption of a 25 s packing time. Bead solution,  $5.4 \times 10^3$  beads/ $\mu\text{L}$ ; flow rate for packing beads,  $10.0 \mu\text{L}/\text{min}$ .

(25) Holden, M. A.; Kumar, S.; Beskok, A.; Cremer, P. S. *J. Micromech. Microeng.* **2003**, *13*, 412–418.

(26) Calculated from the binding capacity ( $0.021 \mu\text{g}$  of biotin-FITC/mg of microbeads), molecular mass of biotin-FITC (831 Da), and number of beads per gram ( $1.829 \times 10^9$ ). These values are provided by the manufacturer.

(27) From the calculated surface area ( $1.5 \times 10^{-13}$  cm<sup>2</sup>/probe, width  $\times$  length) to accommodate a 22-mer duplex DNA based on the size of the duplex having length of 3.4 nm/10 bases and diameter of 2.0 nm.

(28) Watson, J. D.; Crick, F. H. C. *Nature (London)* **1953**, *171*, 737–738.

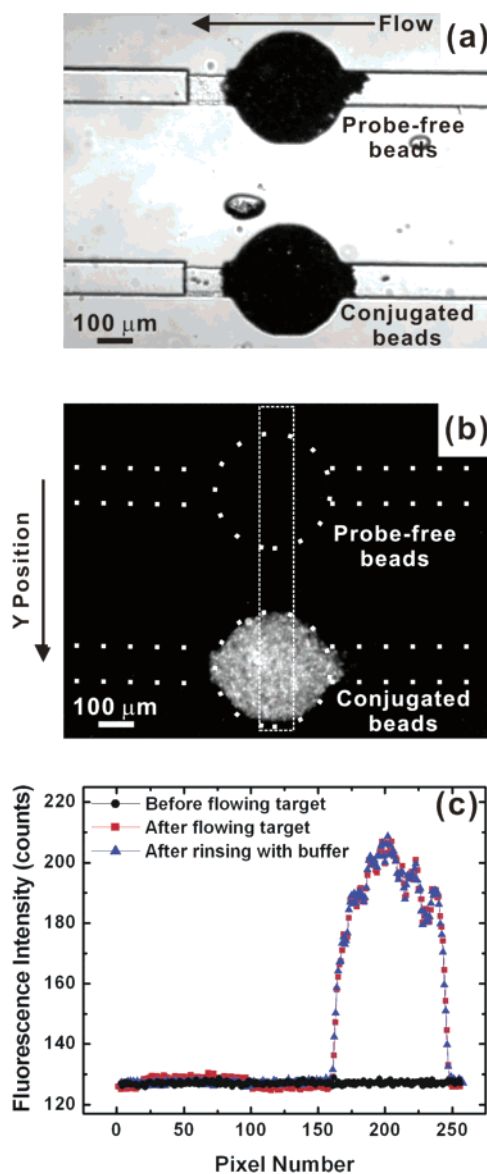


**Figure 2.** (a) Optical micrograph of a two-chamber microfluidic device packed with probe-free microbeads (top chamber) and probe-conjugated microbeads (bottom chamber). (b) Fluorescence micrograph of the two microchambers after exposure to a fluorescently labeled DNA target. Experimental conditions: a  $1.0 \mu\text{M}$  target solution was flowed for 10 min at a rate of  $1.00 \mu\text{L}/\text{min}$  and then the microchannels were rinsed with buffer for 10 min at a flow rate of  $1.00 \mu\text{L}/\text{min}$ . (c) Fluorescence intensity profiles obtained in the regions defined by the dashed white box in Figure 2b.

should be minimal on the microbead surface. This conclusion is consistent with previous reports;<sup>16,17</sup> for example, it has been reported that rapid hybridization occurs on surfaces for probe densities  $< \sim 3 \times 10^{12}$  molecules/cm<sup>2</sup>.<sup>19,17</sup>

**DNA Hybridization.** To confirm hybridization of DNA onto the probe-conjugated microbeads and to evaluate the extent of nonspecific adsorption, a microfluidic device having two independent microchambers was prepared. Probe-free microbeads were packed in one chamber and probe-conjugated microbeads were packed in the other (Figure 2a), and then a  $1.0 \mu\text{M}$  solution of the fluorescein-labeled complement of the probe was simultaneously pumped into both microchambers. After the chambers were rinsed with TAE buffer, significant fluorescence was observed only from the microchamber packed with the probe-conjugated microbeads (Figure 2b). Fluorescence intensity profiles for the region contained within the dashed white box in



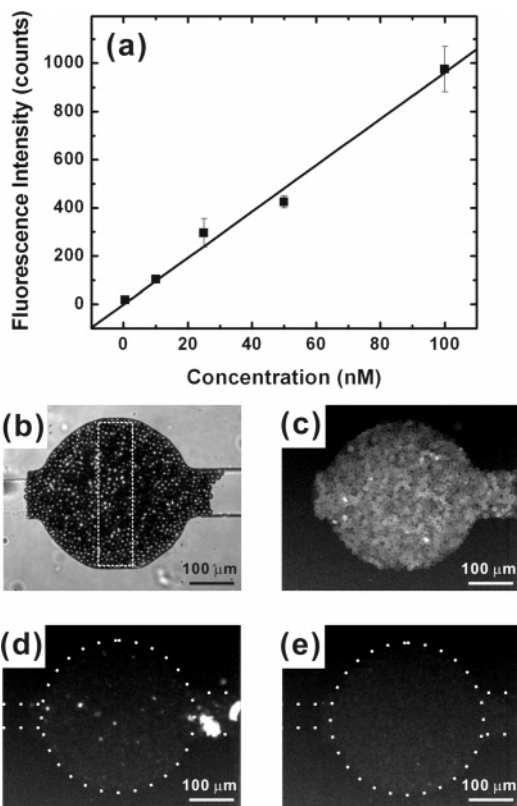


**Figure 3.** Hybridization of DNA onto probe-conjugated microbeads as a function of target solution concentration. (a) Fluorescence intensities obtained in the center region of the microchambers (indicated by the dashed white box in panel b) as a function of target solution concentration. (b) Optical micrograph of a microchamber. (c) Fluorescence micrograph after flowing of complementary DNA target solution (0.5 nM) and rinsing. (d) Fluorescence micrograph after flowing of noncomplementary target solution (100.0 nM) and rinsing. The bright spots near the inlet were impurities observed in a corresponding optical micrograph. (e) Fluorescence micrograph after flowing of buffer solution only. Experimental conditions: target solution was flowed from right to left for 4 min at a flow rate of  $0.50 \mu\text{L}/\text{min}$  and then the microchannels were rinsed for 10 min at a flow rate of  $1.00 \mu\text{L}/\text{min}$ .

Figure 2b are shown in Figure 2c. The data indicate that, after rinsing, the extent of nonspecific binding of the target to the probe-free beads is below the detection limit of the measurement system. Similar experiments were carried out to ensure the absence of nonspecific adsorption on the PDMS and glass surfaces of the microfluidic device (Supporting Information, Figure S2). The stability of the probe/target hybrid was investigated by measuring target fluorescence after the microbeads were rinsed with buffer for 10–30 min. The results (Supporting Information, Figure S3) indicate no detectable change in the extent of hybridization within this time interval.

Hybridization experiments were carried out in the bead-based microfluidic system at concentrations of fluorescently labeled targets ranging from 0.5 to 100.0 nM. Fluorescence intensities as a function of target concentration, obtained from the center region of the microchambers, are plotted in Figure 3a. The target solutions were flowed at  $0.50 \mu\text{L}/\text{min}$  for 4 min, and fluorescence intensities were measured after rinsing for 10 min. Figure 3b is an optical micrograph showing the region of the microchamber used to obtain the fluorescence results. The data in Figure 3a were corrected by subtracting the fluorescence intensity from the center region of the microchamber prior to filling with the target solution. The limit of detection (LOD), defined as the concentration corresponding to a signal 3 standard deviations

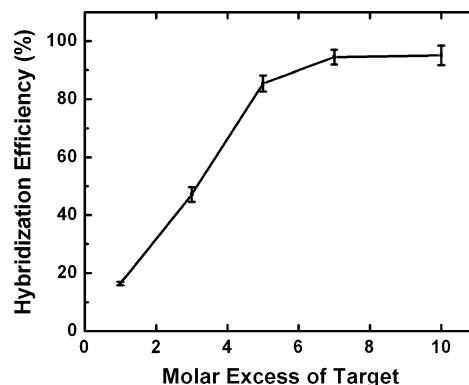


**Figure 4.** Hybridization efficiency as a function of the molar excess of target flowed over the bead bed at a fixed flow rate ( $0.25 \mu\text{L}/\text{min}$ ). The molar excess is given in terms of the ratio of total moles of target DNA flowed per total moles of immobilized probe. The concentration of the target solution was 50.0 nM, and the amount of target DNA was controlled by varying the duration of the exposure. After exposure to the target, the microchannels were rinsed for 10 min at a flow rate of  $1.00 \mu\text{L}/\text{min}$ .

above the zero-concentration blank solution, was found to be  $\sim 10^{-10} \text{ M}$  or  $\sim 10^{-16} \text{ mol}$  of target based on the sample volume of  $\sim 2.0 \mu\text{L}$ . Figure 3c,d demonstrates the selectivity of the assay. Figure 3c was obtained with a 0.5 nM complementary target DNA solution, and Figure 3d was obtained under identical conditions but with a 100.0 nM noncomplementary DNA target solution. Figure 3e represents a control experiment obtained with buffer solution only (zero concentration of DNA). The selectivity ratio, defined as the ratio of fluorescence intensities obtained with complementary and noncomplementary targets present at the same concentration (and with all other conditions identical), is  $> 7.9 \times 10^3$  at 100.0 nM. Despite the simplicity of the microfluidic architecture used for these experiments, the resulting performance specifications (LOD, analysis time, and specificity) are comparable to those for more complex methods such as electric-field-assisted DNA hybridization,<sup>29</sup> other bead-based DNA methods,<sup>7–10</sup> and mixing-assisted DNA hybridization.<sup>30,31</sup>

In addition to determining fluorescence intensities as a function of DNA concentration, we also examined hybridization efficiency as a function of the total moles of target exposed to the microbeads relative to the number of surface-immobilized probes (Figure 4). In this experiment, the target concentration and flow rate were fixed at 50.0 nM and  $0.25 \mu\text{L}/\text{min}$ , respectively, and the moles of target solution passed through the microchamber were controlled by varying the exposure time between 110 and 1100 s. As discussed in the Experimental Section, hybridization efficiency (Figure 4) is defined as the normalized fluorescence intensity for a particular experiment to the limiting fluorescence intensity obtained upon exposure of the probe-modified beads to a high concentration ( $1.0 \mu\text{M}$ ) of target DNA for an extended period of time (10 min). The results indicate that hybridization efficiency reaches a maximum value of  $\sim 90\%$  after exposure of the beads to a 7-fold molar excess of target. Another way of viewing this is that  $\sim 15\%$  of the DNA in this sample is captured in  $\sim 13$  min. This hybridization response can be understood in terms of the good mass transfer characteristics of the microfluidic channel, the high surface-area-to-volume ratio of the microbeads, and the capture-probe surface density. For example, the microbeads are packed very close together, thus decreasing the diffusive

(29) Edman, C. F.; Raymond, D. E.; Wu, D. J.; Tu, E.; Sosnowski, R. G.; Butler, W. F.; Nerenberg, M.; Heller, M. *Nucleic Acids Res.* **1997**, *25*, 4907–4914.

(30) Liu, Y.; Rauch, C. B. *Anal. Biochem.* **2003**, *317*, 76–84.

(31) Yuen, P. K.; Li, G.; Bao, Y.; Müller, U. R. *Lab Chip* **2003**, *3*, 46–50.

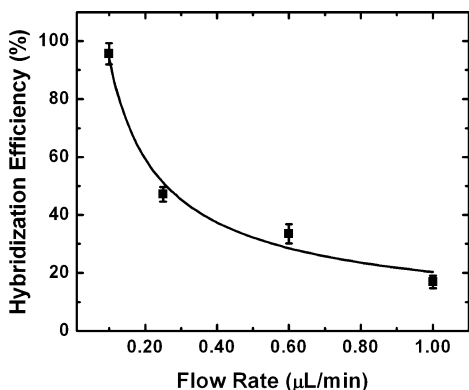


**Figure 5.** Hybridization efficiency as a function of flow rate for a fixed amount of target DNA. For all flow rates, the amount of target DNA represented a 3-fold molar excess relative to the amount of immobilized probe DNA. The number of moles of target DNA was controlled by varying the flow time. After flowing of the target solution (50.0 nM), the microchannels were rinsed for 20 min with buffer. The solid line is the best nonlinear fit to the data by use of Origin software.

transport time of targets from the bulk to the probe surface.<sup>32</sup> This is because the solution volume in the bead bed (0.45 nL) is about 3 times smaller than that of the open microchamber (1.5 nL).<sup>33</sup> In addition, the high surface-area-to-volume ratio of microbeads provides a higher probe surface area ( $6.2 \times 10^5 \mu\text{m}^2$ ) compared to the open microchamber ( $0.71 \times 10^5 \mu\text{m}^2$ ).<sup>34</sup>

Figure 5 is a plot of hybridization efficiency as a function of flow rate for a fixed amount of target DNA passed through the probe-labeled bead bed. In these experiments the number of moles of target presented to the beads was 3 times that of the immobilized probes. The flow rate was varied from 0.10 to 1.00  $\mu\text{L}/\text{min}$ , which corresponds to times ranging from 830 to 83 s, respectively. After flowing of the target solution at a specific rate, the microchamber was rinsed with TAE buffer for 20 min at the same flow rate. Even at the lowest flow rate (0.10  $\mu\text{L}/\text{min}$ ), rinsing for 20 min with buffer was sufficient to displace the solution of target DNA from the channel (Supporting Information, Figure S4).

Figure 5 shows that hybridization efficiency increases as the flow rate decreases. This observation can be understood in terms

(32) Verpoorte, E. *Lab Chip* **2003**, *3*, 60N–68N.

(33) Calculated solution volume of bead bed (solution volume in the open chamber – total bead volume in the chamber) and of the open microchamber ( $\pi \times \text{radius}^2 \times \text{channel height}$ ). Total bead volume in the chamber, 1.03 nL; radius of the chamber, 150  $\mu\text{m}$ ; channel height, 21  $\mu\text{m}$ .

(34) Calculated total surface area of all beads in the microchamber (surface area per bead  $\times$  number of beads) and bottom surface area of the open microchamber ( $\pi \times \text{radius}^2$ ). Probes are assumed to be immobilized only on the bottom surface of the open chamber. Surface area per bead, 311.0  $\mu\text{m}^2/\text{bead}$ ; number of beads in the chamber,  $2 \times 10^3$  beads; radius of the chamber, 150  $\mu\text{m}$ .

of the increase in the flux of target onto the probe-conjugated microbeads at lower flow rates. This observation is consistent with others showing that the flux of analyte to an active surface is inversely proportional to flow rate in fluidic channels.<sup>35,36</sup> For example, theory and experiments indicate that flux is proportional to  $q^{-2/3}$  ( $q$  is the flow rate in units of meters per second) under mass-transfer-limited reaction conditions and to  $q^{-1}$  under kinetically limited conditions.<sup>36</sup> Consistent with these earlier findings, the best fit to the data in Figure 5 (solid line) is proportional to  $q^{-2/3}$ .

## Summary and Conclusions

We have described a simple microfluidic device packed with microbeads conjugated to DNA capture probes and the parameters that affect its performance. These include target concentration, probe surface concentration, and flow rate. The inherently high surface-area-to-volume ratio of microbeads, coupled with their close proximity, leads to efficient target capture. Specifically, the microfluidic device has an LOD of  $\sim 10^{-10}$  M ( $\sim 10^{-16}$  mol) and a selectivity factor greater than  $7.9 \times 10^3$ . Analysis times are typically on the order of a few minutes.

We recently reported a simple means for enhancing the local concentration of DNA in microfluidic systems by a factor of up to  $\sim 500$  within 150 s.<sup>37</sup> At present, we are integrating this preconcentrator into a bead-based capture chip similar to that described here. Through this and other improvements, we expect that bead-based microfluidic devices of this sort will ultimately have significantly lower LODs, faster analysis times, and parallel detection capabilities that may make them viable tools for gene expression studies, clinical diagnostics, and high-throughput drug screening.

**Acknowledgment.** Financial support from the Texas Institute for Intelligent Bio-Nano Materials and Structures for Aerospace Vehicles, funded by NASA Cooperative Agreement NCC-1-02038, is gratefully acknowledged.

**Supporting Information Available:** A movie showing the microbead packing process, a calibration curve obtained with solution-phase (no microbeads) ssDNA probes modified with fluorescein and biotin, and fluorescence intensity profiles indicating no significant nonspecific adsorption of targets and stability of hybridized targets during rinsing. This material is available free of charge via the Internet at <http://pubs.acs.org>.

LA0616956

(35) Weber, S. G.; Purdy, W. C. *Anal. Chim. Acta* **1978**, *100*, 531–544.

(36) Sjölander, S.; Urbaniczky, C. *Anal. Chem.* **1991**, *63*, 2338–2345.

(37) Dhopeswarkar, R.; Sun, L.; Crooks, R. M. *Lab Chip* **2005**, *5*, 1148–1154.